Angular distributions of the ^{6}Li(n,t)^{4}He and ^{10}B(n,α)^{7}Li reactions at 2 and 24 keV

M. L. Stelts, R. E. Chrien, M. Goldhaber, and M. J. Kenny

Brookhaven National Laboratory, Upton, New York 11973

C. M. McCullagh

State University of New York, Stony Brook, New York 11794

(Received 1 November 1978)

The angular distributions of charged particles from the ^{6}Li(n,t)^{4}He and ^{10}B(n,α)^{7}Li were measured with monoenergetic neutron beams from a reactor. Silicon surface barrier detectors were used. The ^{6}Li(n,t)^{4}He data were compared with previous results having poorer angular resolution and with an R-matrix calculation. The ^{10}B(n,α)^{7}Li data show a marked anisotropy at 2 and 24 keV for the ground state group and a lesser anisotropy for α's leading to the first excited state of ^{7}Li. Branching ratios are measured at thermal, 2- and 24-keV neutron energies. The results are compared with the R-matrix calculation.

INTRODUCTION

The ^{6}Li(n, t)^{4}He and the ^{10}B(n, α)^{7}Li reactions have been used in the measurement of neutron fluxes for many years.[1-6] The relatively high Q values, ease of detection of the reaction products, and the rather high cross sections with relatively smooth dependence on incident neutron energy make these reactions very convenient for monitoring neutron fluxes for neutron energies less than a few hundred keV. Consequently, considerable effort has been devoted to measuring these cross sections to an accuracy of a few percent.[7-11]

Measurements of various reaction cross sections leading to the same compound nuclear states in ^{7}Li and ^{11}B have been made at various laboratories. It is therefore useful to develop a self-consistent R-matrix calculation[12,13] which can generate a global fit to all these data. Measurements of the angular distributions can help to reduce the ambiguity of these fits. Anisotropies of the angular distribution can also affect the response of detectors of finite size through varying wall effects and detection efficiency as the distribution changes with energy. Therefore it is valuable to know the angular distributions for these reactions.

The angular distributions produced by very low energy neutrons are expected to be isotropic because of the dominance of s-wave neutrons in the entrance channels. Recently experiments[14-17] below 100 keV with the ^{6}Li(n, t)^{4}He reactions have measured sizable anisotropies for incident neutron energies of 24 keV or less. The experiments below 50 keV had rather poor angular definition, (solid angle $\gtrsim \pi$ sr). The anisotropy is ascribed to s-p wave interference. There are no reported

measurements of the ^{10}B(n, α)^{7}Li angular distribution below 200 keV. Because of the intense quasi-monoenergetic beams at 2 and 24 keV available from the tailored beam facility[18] at the Brookhaven High Flux Beam Reactor, it is possible to make these measurements with good angular resolution. We therefore remeasured the anisotropy of the ^{6}Li(n, t)^{4}He reaction and measured the angular distribution of the ^{4}He's leading to the ground and first excited states of ^{7}Li in the ^{10}B(n, α)^{7}Li reaction.

EXPERIMENTAL APPARATUS

The angular distributions were measured at the tailored beam facility at the HFBR in a 31-cm diameter evacuated scattering chamber using two silicon surface barrier detectors to detect the reaction products. The tailored beam facility uses the selective neutron transmission properties of bismuth single crystals, scandium, and isotopic ^{56}Fe to produce neutron beams of thermal, 2- and 24-keV energy, respectively. The energy resolution of the 2- and 24-keV beams is about 900 eV. The thermal neutron flux is about 10^8 n/cm^2 s. The fluxes of the 2- and 24-keV beams are each about 10^7 n/cm^2 s. The beams are collimated with borated nylon collimators. The experimental setup is shown in Fig. 1.

The two detectors were 300-μm thick silicon surface barrier detectors. The bias voltage was chosen to select a depletion depth sufficiently thick to stop the charged particles from the reaction but thin enough to minimize the energy deposited by fast electrons. The detectors were placed in a cylindrical holder with a defining col-
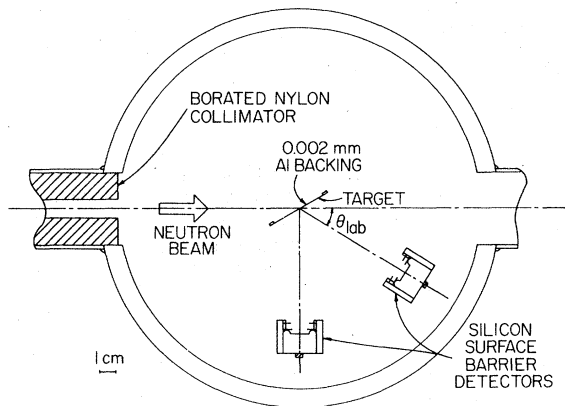
FIG. 1. Experimental apparatus showing scattering chamber with typical orientation of neutron beam, target, and detectors.

limator and antiscattering collimator as shown in Fig. 1. The defining collimator was 10.3 mm in diameter. The detectors were mounted so that the defining collimator was about 79 mm from the center of the chamber. The distances from the center of the chamber to the defining collimator were measured to an accuracy of ~0.05 mm.

Alignment of the center of the beam was carried out using two 3.175-mm collimators placed 1 m apart. The neutron beam transmission through the collimators was monitored by a ^{235}U fission chamber. A 0.5-cm-thick polyethylene scatterer was placed between the exit collimator and the fission chamber to minimize any effects due to detector nonuniformity. The axis of the collimators was then adjusted to maximize the counting rate. Finally a telescope was centered on this axis to define the beam line. The accuracy of alignment at the center of the chamber is estimated at ±1.5 mm.

The resolution of the charged particle groups is limited almost entirely by their energy loss in the target. Therefore, to make the energy loss at the two angles as nearly equal as possible, the target was oriented so that the normal to the target plane would bisect the angle between the two detectors.

The signals from the detectors were amplified by charge sensitive preamplifiers and shaped by double delay line main amplifiers. A Northern Scientific NS459A Router with a NS625 analog-to-digital converter (ADC) was used to store the pulse height spectra simultaneously into separate 512 channel subgroups in an SDS910 computer. The spectra were stored on magnetic tape for subsequent off-line analysis.

EXPERIMENT

The primary object of the experiment is to measure a relative $[d\sigma/d\Omega(\theta)]_{c.m.}$ for the ^{6}Li$(n, t)^4$He, the ^{10}B$(n, \alpha_0)^7$Li, and the ^{10}B$(n, \alpha_1)^7$Li* reactions. We chose to normalize the angular distribution so that $[d\sigma/d\Omega(90°)] = 1$. We therefore made all measurements in pairs with one detector fixed at 90° and the other at angle θ. To make an accurate comparison of the cross section at the two angles it proved necessary to fully resolve the reaction products and to accurately know the relative solid angles of the two detectors.

Sample thermal spectra are shown in Figs. 2 and 3. Figure 2 shows the spectra of triton and ^{4}He particles from the ^{6}Li$(n, t)^4$He reaction for a 199-μg/cm^2 target. (The thicknesses of all targets were determined by measuring the widths of the peaks and using the energy loss tables of Ref. 19. The estimated uncertainty of the thickness is ≲10%.) The triton and α groups are clearly
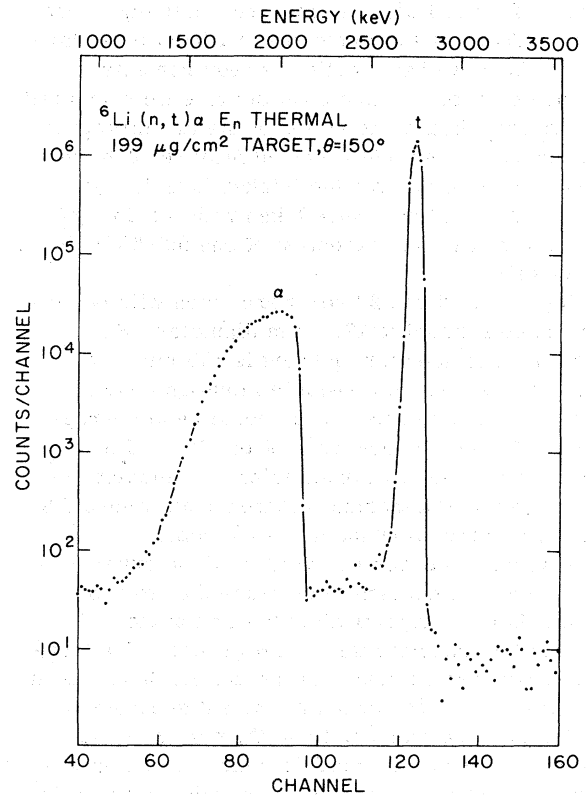

FIG. 2. Spectrum of charged particles emitted in the ^{6}Li$(n, t)^4$He reaction at thermal neutron energy. The widths of the t and α peaks are ascribed to energy loss of the charged particles in the target.
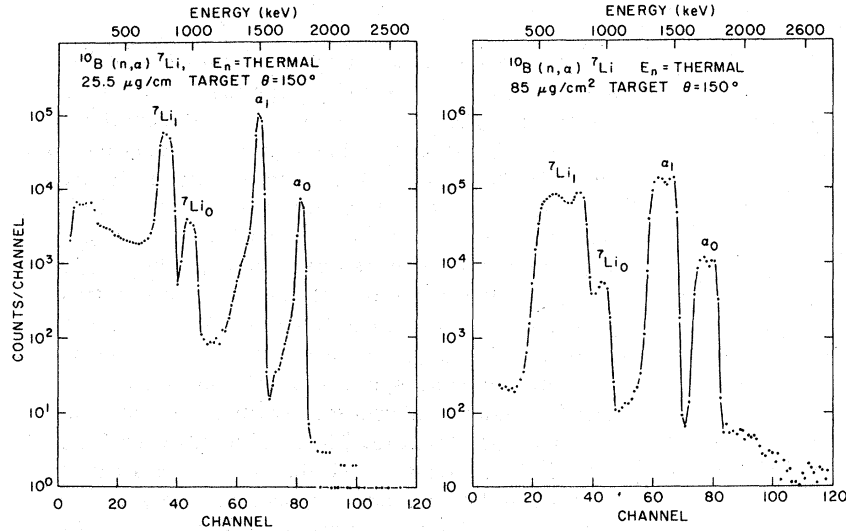
FIG. 3. Spectra of charged particles from the 25.5- and 85-μg/cm^2 ^{10}B targets at thermal neutron energy.

resolved. For the ^{10}B$(n,\alpha)^7$Li reactions two targets of 25.5 and 85.0 μg/cm^2, respectively, were used. Figure 3 shows the spectra from these targets. Since we had conflicting requirements of adequate resolution and counting rate we compared the thermal branching ratios of the two targets to assure ourselves that we could fully resolve the α_0 and α_1 groups from the thicker target. All data at 2 and 24 keV were taken with the 85-μg/cm^2 target with the exception of one 90°-60° pair at 24 keV.

The data at 2 and 24 keV were taken with neutron beams collimated to 12.7-mm diameter. Since the target to detector distance is ~79 mm, we were concerned with possible misalignments, target nonuniformities, and geometrical corrections affecting the accuracy of the data. These can be overcome by normalizing the detector efficiencies with a thermal neutron beam where the angular distribution should be isotropic.

However, to check the validity of the experimental method we decided to measure the isotropy of the thermal angular distribution for the ^{10}B$(n,\alpha)^7$Li reaction for both α groups. The thermal beam was defined with the two 3.175-mm collimators with an estimated alignment accuracy of ±0.8 mm. The distance from the center of the chamber to each detector defining collimator was measured to ±0.05 mm. If the angular distribution is expressed as a sum of Legendre polynomials with no more than second order terms, then the results of these measurements (made at angles from 15° to 150°) indicate that the angular aniso-
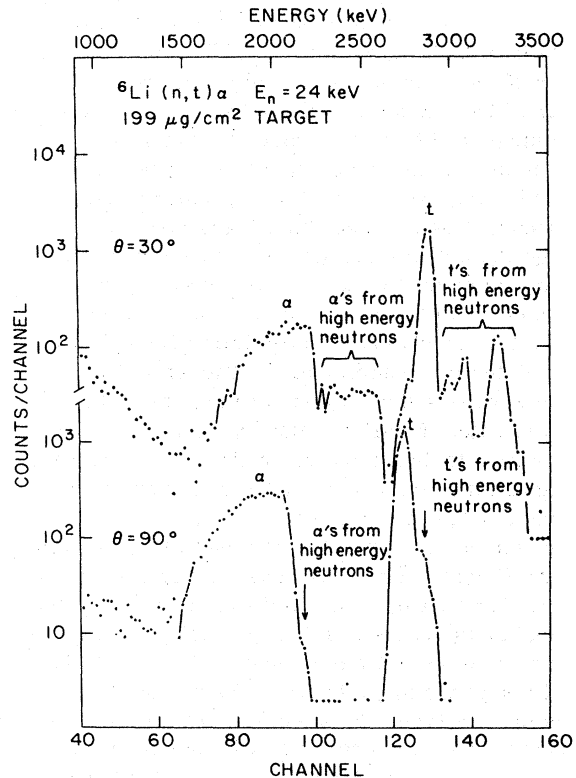

FIG. 4. Spectra of charged particles from the ^{6}Li target at 30° and 90° for 24-keV incident neutron energy. Those particle groups due to higher energy incident neutrons are indicated.
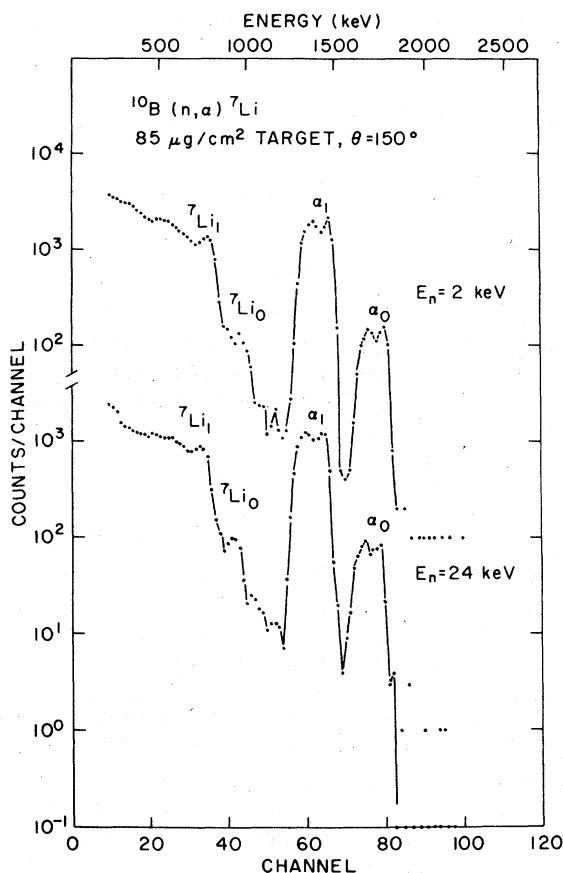
FIG. 5. Typical spectra of charged particles from the 85-μg/cm^2 ^{10}B target at 2 and 24 keV.

tropy at thermal neutron energy is less than 2%. This measured deviation from isotropy can be explained by uncertainties in geometrical alignment.

Since the ^{7}Li$_0$ and ^{7}Li$_1$ groups are also clearly resolved for the 25.5-μg/cm^2 target and since

$$\left[\frac{d\sigma}{d\Omega}(\theta)\right]_{^7\text{Li}} = \left[\frac{d\sigma}{d\Omega}(180°-\theta)\right]_\alpha ,$$

it is possible to compare the angular distribution at θ and $(180°-\theta)$ within the same spectrum and thus avoid any geometrical effects. These ratios provide the constraint that any odd Legendre terms contribute less than a few tenths of a percent to the distribution. Consequently we make the assumption in the analysis of the 2- and 24-keV measurements that the thermal angular distribution is isotropic and we normalize our data to thermal isotropy.

The spectra of the ^{6}Li$(n, t)^4$He reaction at 24-keV incident neutron energy are shown in Fig. 4 for angles of 30° and 90°. The peaks at energies higher than the main α and t peaks at 30° are due to groups of neutrons in the incident neutron beam of energies higher than 24 keV. The 2-keV data show similar structure which will be discussed in detail below. Figure 5 shows representative 2- and 24-keV spectra for the ^{10}B$(n, \alpha)^7$Li reaction. The α groups are adequately resolved at both energies.

DATA ANALYSIS AND RESULTS

A. Data analysis

The angular distributions at angle θ are all measured relative to the center-of-mass differential cross section at 90°. Thus we define

$$R_E(\theta) = \frac{[d\sigma/d\Omega(\theta)]_{\text{c.m.}}}{[d\sigma/d\Omega(90°)]_{\text{c.m.}}} , \qquad (1)$$

where E denotes the incident neutron energy. The formula for computing R is as follows:

$$R_E^P(\theta) = \frac{A_E^P(\theta)}{A_E^P(90°)} \frac{A_{\text{th}}^P(90°)}{A_{\text{th}}^P(\theta)} \frac{K_E^P(\theta)}{K_E^P(90°)} . \qquad (2)$$

$A_E^P(\theta)$ is the area of the peak for the selected particle P at angle θ due to incident neutrons of energy E. $K_E^P(\theta)$ is the solid angle factor for converting from the laboratory to center-of-mass system:

$$K_E^P(\theta) = \frac{[\Delta\Omega(\theta)]_{\text{lab}}}{[\Delta\Omega(\theta)]_{\text{c.m.}}} . \qquad (3)$$

If the associated particle P' in the reaction is resolved at angle θ then the cross section ratio at $\theta' = (180°-\theta)$ can be computed as

$$R_E^P(\theta') = \frac{A_E^{P'}(\theta)}{A_E^{P'}(90°)} \frac{A_{\text{th}}^{P'}(90°)}{A_{\text{th}}^{P'}(\theta)} \frac{K_E^{P'}(\theta)}{K_E^{P'}(90°)} . \qquad (4)$$

The change in angle in converting from laboratory to center-of-mass coordinates was sufficiently smaller than the angular resolution of these measurements that it was ignored.

The kinematic calculations were performed using standard nonrelativistic formulation. It should be noted that the center-of-mass motion causes rather large changes in the final particle energies and solid angle ratios as a function of angle at fairly low neutron energies. For example, at 24 keV there is a 10% difference in the energy of the α_0 group from the ^{10}B$(n, \alpha)^7$Li reaction between 0° and 180°. The solid angle ratio for this group differs by 13% between forward and backward directions. These effects, by themselves, can cause significant deviations in detector response as a function of neutron energy.

Figure 4 shows clearly the presence of small but significant higher energy neutron groups in the 24-keV beam. The 2-keV data show similar structure. The triton energy resolution and dispersion with neutron energy is sufficient that the strength of the group due only to the principal neutron energy group in the beam can be extracted. For the ^{10}B$(n, \alpha)^7$Li this is not the case and corrections must be made for the unresolved α's.

The corrections were made in the following manner: It was decided to approximate the high energy groups by 2 groups at 60 and 240 keV for the 2-keV neutron beam and by 2 groups at 100 and 240 keV for the 24-keV beam. ^{6}Li$(n, t)^4$He cross sections and angular distributions were taken from the literature.[7,10] Kinematic factors were applied to extract a relative $d\sigma/d\Omega$ at 30° in the laboratory system for the appropriate energies. The relative fluxes at energies E and E_b can now be determined using

$$\frac{\varphi(E)}{\varphi(E_b)} = \frac{C(E)}{C(E_b)} \frac{\sigma(E_b)}{\sigma(E)},$$

where $C(E)$ are the counts in the spectrum at neutron energy E, σ is the cross section, and E_b is the primary beam energy.

For the 2-keV beam the relative fluxes are 10.4% at ~60 keV and 3.2% at ~240 keV. For the 24-keV beam 8.7% at ~100 keV and 1.8% at ~240 keV.

Consideration of the kinematics, regions of integration in the spectra, and the cross sections for the ^{10}B$(n, \alpha_{0,1})^7$Li reactions leads to relationships for the total counting rate for each α group as a function of angle and high energy contaminants E_1, E_2; e.g., for 30°, 2 keV, 0 = gs group:

$$C_T^0(30°) \propto A_2^0(30°) \left(1 + \frac{\sigma_{E1}^0}{\sigma_2^0} \frac{\varphi_{E1}}{\varphi_2} + \frac{\sigma_{E2}^1}{\sigma_2^0} \frac{\varphi_{E2}}{\varphi_2}\right),$$

where C is the expected number of counts, the φ, σ are the appropriate fluxes and cross sections, and $A_2^0(30°)$ [$\propto \sigma_2^0(30°)\varphi$] is the area expected from the g.s. cross section for 2-keV neutrons. By

taking the appropriate ratios the following correction factors are derived:

$$\frac{A_E^0(\theta)}{A_E^1(\theta)} = G_E(\theta) \frac{C_T^0(\theta)}{C_T^1(\theta)}, \tag{5}$$

$$\frac{A_E^0(\theta)}{A_E^0(90°)} = H_E(\theta) \frac{C_T^0(\theta)}{C_T^0(90°)}, \tag{6}$$

$$\frac{A_E^1(\theta)}{A_E^1(90°)} = I_E(\theta) \frac{C_T^1(\theta)}{C_T^1(90°)}. \tag{7}$$

$A_E^P(\theta)$ is the part of the area of the peak due to neutrons of energy E at angle θ for α groups P = 0, 1. None of these coefficients differs from 1.00 by more than 7%. These factors are then used to compute the ratio of areas used in Eq. (2) for the ^{10}B$(n, \alpha)^7$Li data.

B. Results—angular distributions

All the data for the ^{6}Li$(n, t)^4$He reaction were taken with a 199-μg/cm^2 target. The time necessary to accumulate the spectra at 2 or 24 keV for a given pair of angles ranged from 1400 to 2600 minutes. The data for the ^{10}B$(n, \alpha)^7$Li reaction were taken (with one exception) with an 85-μg/cm^2 target. Running times varied from 1200 to 6488 minutes. The 25.5-μg/cm^2 target was run for 4600 minutes to get a 60°-90° pair at 24 keV to check on the corrections used for high energy neutron groups for the ^{10}B$(n, \alpha)^7$Li reaction. For the ^{6}Li$(n, t)^4$He reaction at the angle θ, the angular distribution from the triton can be calculated directly from the triton peak $A_E^t(\theta)$ or from the α peak at the associated particle angle (180° − θ), $A_E^\alpha(180 - \theta)$. These results, together with their averages, are summarized in Table I. The consistency of the results obtained with both α's and t's is good. These results are shown in Fig. 6.

The angular distributions for the ^{10}B$(n, \alpha)^7$Li reaction are summarized in Table II. These results are plotted in Fig. 7 for the α_0 and α_1 groups. The deviation of the results for the different runs was within the statistical uncertainty.

TABLE I. Center-of-mass angular distributions for the ^{6}Li$(n, t)^4$He reaction (ratios to the 90° differential cross section).

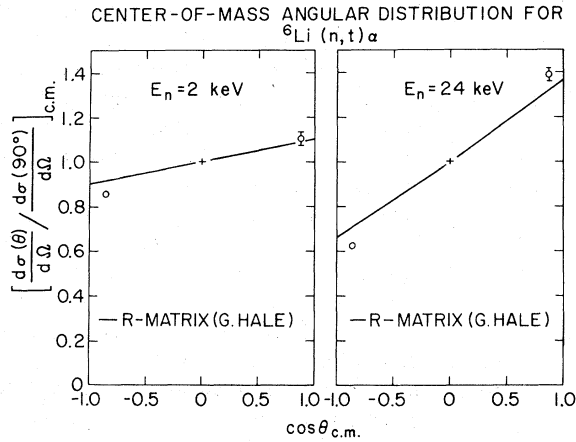| E_n (keV)	θ	$R_E^t(\theta)$ from t peak	$R_E^t(\theta)$ from α peak	$\langle R_E^t(\theta)\rangle$
2	30°	1.080(11)	1.153(34)	1.104(30)
	150°	0.860(12)	0.844(23)	0.855(10)
24	30°	1.340(29)	1.438(47)	1.389(30)
	150°	0.626(15)	0.626(23)	0.626(14)

CENTER-OF-MASS ANGULAR DISTRIBUTION FOR
^{6}Li (n,t)α

FIG. 6. The center-of-mass angular distributions of the tritons from the ^{6}Li$(n,t)^4$He reaction at 2- and 24-keV neutron energy. The distribution is normalized to unity at 90°. The solid lines are the R- matrix calculations of Hale (Ref. 25) using the parameters of the ENDF/B-V evaluation.

C. Results: branching ratios

In the course of making the normalization to thermal neutron energy we collected considerable data on the ratio of the ground state to first excited state transition probabilities for the ^{10}B$(n, \alpha)^7$Li reaction. For the eight spectra taken with the 25.5-μg/cm^2 target (see Fig. 3 for a sample spectrum) we accumulated a total of ~10^5 counts in the α_0 groups. The result of the average over these runs was

$$\alpha_0/\alpha_1 = (6.696 \pm 0.023)\% .$$

Both the statistical error and the mean square deviation was 0.023%. No dependence on the angle of measurement or the detector used was noted.

The data taken with the 85-μg/cm^2 target did not have the resolution of the thinner target but still

CENTER-OF-MASS ANGULAR DISTRIBUTION FOR
^{10}B(n,α_1)^{7}Li*

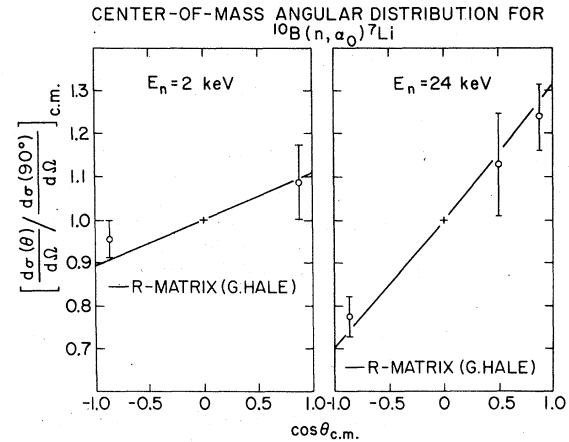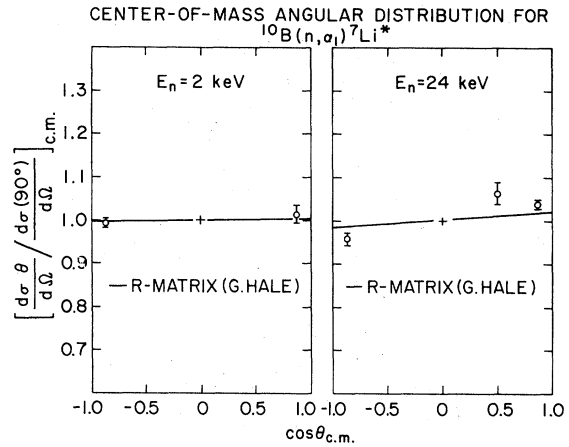CENTER-OF-MASS ANGULAR DISTRIBUTION FOR
^{10}B(n,α_0)^{7}Li

FIG. 7. The center-of-mass angular distributions for the α_0 and α_1 groups from ^{10}B$(n, \alpha)^7$Li reaction at 2- and 24-keV neutron energy. The distributions are normalized to unity at 90°. The solid lines are the R-matrix calculations of Hale (Ref. 25) using the parameters of the ENDF/B-V evaluation.

had peak to valley ratios of better than 2 orders of magnitude for the α_0 group and 3 orders of magnitude for the α_1 group. The results averaged over 10 spectra were

$$\alpha_0/\alpha_1 = (6.699 \pm 0.012)\%$$

with the mean square deviation again the same as the statistical error. Again, no dependence on angle or detector was observed. The total counts in the α_0 group was ~7×10^5. The most precise of previous experiments[20-24] with which to compare is that of Deruytter and Pelfer.[24] They measured (with statistics of 10^6 counts in the α_0 peak) a value of (6.733 ± 0.008%). Although we agree to 0.034%, there is still a difference of about 3 standard deviations between these results.
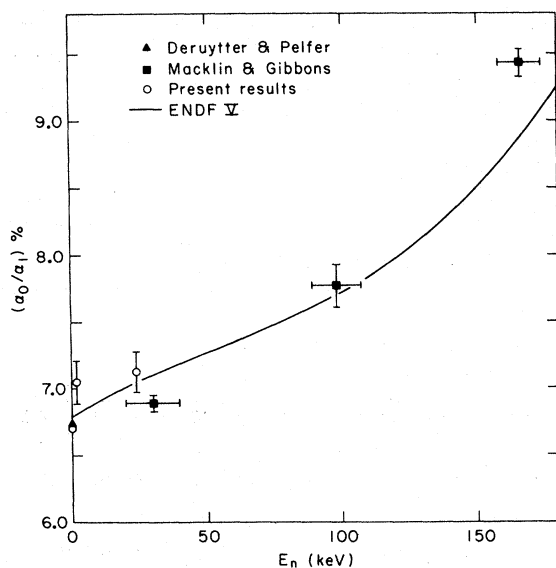
TABLE II. Center-of-mass angular distributions for the ^{10}B$(n, \alpha_0)^7$Li and ^{10}B$(n, \alpha_1)^7$Li reactions (ratios to the 90° differential cross section).

E_n (keV)	θ	$R_E^{\alpha_0}(\theta)$	$R_E^{\alpha_1}(\theta)$
2	30°	1.087(86)	1.017(21)
	150°	0.955(43)	0.993(12)
24	30°	1.24(8)	1.037(11)
	60°	1.13(12)	1.064(26)
	150°	0.772(46)	0.958(14)

FIG. 8. The branching ratios (α_0/α_1) for the ^{10}B$(n, \alpha)^7$Li reaction as function of neutron energy. The present results are indicated by the circles. The triangle is the data point from Deruytter and Pelfer (Ref. 24). The squares are the data from Macklin and Gibbons (Ref. 23). The solid line is the ENDF/B-V evaluation.

and Pelfer have marginally better statistics with resolution and background similar to our experiment. However, we have used two different detectors, two different targets, and three different angles in accumulating our data. The results were internally consistent. The data points indicated by the squares are those of Macklin and Gibbons.[23] They used a pulsed Van de Graaff and a ^{7}Li target to generate neutrons and back to back solid state detectors to measure the α_0/α_1 ratios. The solid curve is the (Evaluated Nuclear Data File—version B-V) ENDF/B-V evaluation. The data seem reasonably consistent.

The 24-keV angular distribution for ^{6}Li$(n, t)^4$He can be compared with the data of Schroder et al.[15] and Raman et al.[16,17] This comparison is made in Fig. 9. Our data points are the circles, the cross-hatched histograms the data of Schroder et al., and the squares the values of Raman et al. at 24 keV. The angular resolution is indicated by the horizontal bars. The experiment of Schroder et al. was done with the 24-keV Fe filter beam at NBS. Because of the low counting rate the experiment was done with ~2π solid angle for each detector.
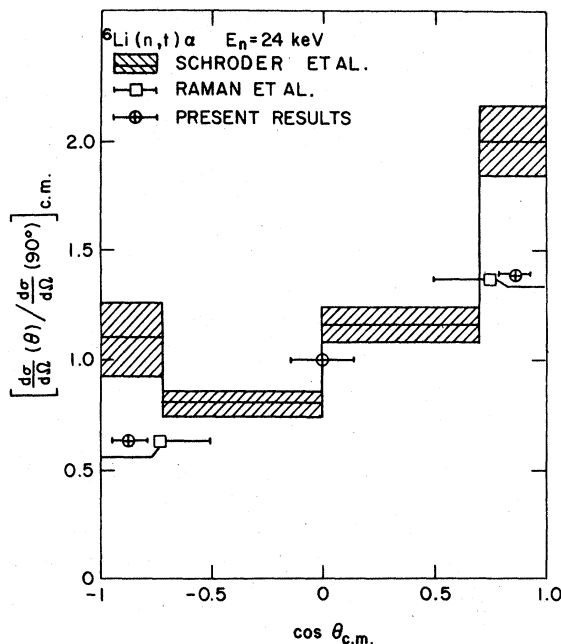
For neutrons of 2 and 24 keV, branching ratio measurements become somewhat more difficult, both from the poorer statistics and higher backgrounds at these energies and from the fact that the angular distributions are different for each α group. Since the distributions are found to follow an $a + b\cos\theta$ dependence, the 90° data will give the most reliable measure of α_0/α_1. An average of the 30° and 150° points should lead to the same results. A weighted average of the data gave

$$\alpha_0/\alpha_1 = (7.05 \pm 0.16)\% \text{ at 2 keV}$$

and

$$\alpha_0/\alpha_1 = (7.13 \pm 0.15)\% \text{ at 24 keV.}$$

The corrections for contributions by high energy neutron groups have been applied as previously discussed. These points are plotted as the circles in Fig. 8.

DISCUSSION OF RESULTS

We will first discuss the branching ratio α_0/α_1. The experimental data available below 160 keV are summarized in Fig. 8. At thermal neutron energy, for purposes of plotting, our value and that of Deruytter and Pelfer's[24] coincide though they do differ by 3 standard deviations. Deruytter

FIG. 9. Comparison of the present triton distribution results for the ^{6}Li$(n,t)^4$He reaction with previous data. Our data are the circles. The squares are the data of Raman et al. (Ref. 16) and the histogram the data of Schroder et al. (Ref. 15). The horizontal error bars indicate the angular resolution of the experiments.

By taking coincidence data with the detectors at $0°$ and $45°$ relative to the neutron beam, they extracted the angular distribution given in the figure. The data of Raman et al. were taken at ORELA using the time-of-flight technique with a solid state detector subtending $\approx \pi$ sr solid angle. The forward-backward anisotropy can be found by measuring the ratio of the yield of tritons and α's. Their data are in excellent agreement with the present results.

Hale[12,13,25] provided us with the angular distribution computed by the R-matrix calculations used in evaluation of the ^{7}Li and ^{11}B systems. These are the solid lines in Figs. 6 and 7. These calculations are based on parameters derived from both neutron- and charged particle-induced reactions which involve the relevant states in the compound system. The R-matrix parameters were obtained by least-squares fitting to these previous data sets. No further adjustment of the parameters to fit our data was made. The calculation agrees well with experiment for both the ^{6}Li$(n, t)^4$He and the ^{10}B$(n, \alpha_0)^7$Li reactions. The largest disagreement is for the 24-keV α_1 group. The calculation yields a result somewhat more isotropic than experiment. Even here the disagreement is no more than two standard deviations or about 2%.

CONCLUSIONS

Angular distributions have been measured for the ^{6}Li$(n, t)^4$He and ^{10}B$(n, \alpha)^7$Li reactions at 2- and 24-keV neutron energy with high angular resolu-

tion. The 24-keV ^{6}Li$(n, t)^4$He results are in agreement with the values of Raman et al.[16] and in good agreement with the global R-matrix calculations of Hale.[12,13,25] The ^{10}B$(n, \alpha)^7$Li angular distributions were measured for the first time at these neutron energies. The ground state reaction was shown to be quite anisotropic while the dominant first excited state group is nearly isotropic. The R-matrix calculations of Hale[25] agree with these results.

The branching ratios α_0/α_1 have been measured at thermal, 2 and 24 keV. The results are consistent with previous measurements and in qualitative agreement with the ENDF/B-V evaluation.

These data provide information for precise computation of detector response where ^{6}Li or ^{10}B is used. The agreement with the R-matrix calculations gives more confidence in the use of these calculations in the evaluation and interpolation of the various experimental data in these nuclei.

[1]J. Chadwick and M. Goldhaber, Nature 135, 341 (1935); Camb. Philos. Soc. Proc. 31, 612 (1935).

[2]E. Amaldi, O. D'Agostino, E. Fermi, B. Pontecorvo, F. Rasetti, and E. Segrè, Proc. R. Soc. London A149, 522 (1935).

[3]A. D. Carlson, NBS Special Publication No. 425, edited by R. A. Schrack and C. B. Bowman, 1975 (unpublished), p. 293.

[4]G. P. Lamaze, NBS Special Publication No. 493, edited by C. D. Bowman, A. D. Carlson, H. O. Liskien, and L. Stewart, 1977 (unpublished), p. 37.

[5]L. W. Weston, NBS Special Publication No. 493, edited by C. D. Bowman, A. D. Carlson, H. O. Liskien, and L. Stewart, 1977 (unpublished), p. 43.

[6]A. D. Carlson, NBS Special Publication No. 493, edited by C. D. Bowman, A. D. Carlson, H. O. Liskien, and L. Stewart, 1977 (unpublished), p. 85.

[7]M. S. Coates, G. J. Hunt, and C. A. Uttley, Neutron Standards and Flux Normalization, Conference No. 701002, 1971 (unpublished), p. 121.

[8]S. J. Friesenhahn, V. J. Orphan, A. D. Carlson, M. P. Fricke, and W. M. Lopez, NBS Special Publication No. 425, edited by R. A. Schrack and C. D. Bowman, 1975 (unpublished), p. 232.

[9]J. A. Harvey and N. W. Hill, NBS Special Publication No. 425, edited by R. A. Schrack and C. D. Bowman, 1975 (unpublished), p. 244.

[10]H. Derrien and L. Edvardson, NBS Special Publication No. 493, edited by C. D. Bowman, A. D. Carlson, H. O. Liskien, and L. Stewart, 1977 (unpublished), p. 14.

[11]E. Wattecamps, NBS Special Publication No. 493, edited by C. D. Bowman, A. D. Carlson, H. O. Liskien, and L. Stewart, 1977 (unpublished), p. 67.

[12]G. M. Hale, NBS Special Publication No. 425, edited by R. A. Schrack and C. D. Bowman, 1975 (unpublished), p. 302.

[13]G. M. Hale, NBS Special Publication No. 493, edited by C. D. Bowman, A. D. Carlson, H. O. Liskien, and L. Stewart, 1977 (unpublished), p. 30.

[14]C. Beets, G. DeLeeuw-Gierts, S. DeLeeuw, Y. Baudinet-Robinet, G. Robaye, and L. Winand, Nucl. Phys. 69, 145 (1965).

[15]I. G. Schroder, E. D. McGarry, D. DeLeeuw-Gierts, and S. DeLeeuw, NBS Special Publication No. 425, edited by R. A. Schrack and C. D. Bowman, 1975 (unpublished), p. 240.

[16]S. Raman, N. W. Hill, J. Halperin, and J. A. Harvey,

Proceedings of the International Conference on the Interactions of Neutrons with Nuclei, edited by E. Sheldon (Technical Information Center, ERDA, Lowell, Mass., 1976), p. 1340.

[17]J. A. Harvey and I. G. Schroder, NBS Special Publication No. 493, edited by C. D. Bowman, A. D. Carlson, H. O. Liskien, and L. Stewart, 1977 (unpublished), p. 10.

[18]R. C. Greenwood and R. E. Chrien, Nucl. Instrum. Methods 138, 125 (1976).

[19]L. C. Northcliffe and R. F. Schilling, Nucl. Data Tables A7, 233 (1970).

[20]E. Bujdosó, Nucl. Phys. 6, 107 (1958).

[21]S. Malmskog, Physica 29, 987 (1963).

[22]William M. Toney and Arthur W. Waltner, Nucl. Phys. 80, 237 (1966).

[23]R. L. Macklin and J. H. Gibbons, Phys. Rev. 165, 1147 (1968).

[24]A. J. Deruytter and P. Pelfer, J. Nucl. Energy 21, 833 (1967).

[25]G. M. Hale, private communication.